Biochemical and Biophysical Research Communications 390 (2009) 728–732

Contents lists available at ScienceDirect

Biochemical and Biophysical Research Communications

journal homepage: www.elsevier.com/locate/ybbrc

Organization and dynamics in micellar structural transition monitored by pyrene fluorescence

Arunima Chaudhuri, Sourav Haldar, Amitabha Chattopadhyay *

Centre for Cellular and Molecular Biology, Council of Scientific and Industrial Research, Uppal Road, Hyderabad 500 007, India

ARTICLE INFO

Article history:
Received 1 October 2009
Available online 13 October 2009

Keywords:
Structural transition
Pyrene fluorescence
Rod-shaped micelles
SDS
Ionic strength
Dielectric constant

ABSTRACT

Structural transitions involving shape changes play an important role in cellular physiology. Such transition can be induced in charged micelles at a given temperature by increasing ionic strength of the medium. We have monitored the change in organization and dynamics associated with sphere-to-rod transition of SDS micelles utilizing pyrene fluorescence. We report here, utilizing changes in the ratio of pyrene vibronic peak intensities (I_1/I_3), the apparent dielectric constant experienced by pyrene in spherical SDS micelles (in absence of salt) to be ~32. Interestingly, the apparent micellar dielectric constant exhibits a reduction with increasing NaCl concentration. The dielectric constant in rod-shaped micelles of SDS (in presence of 0.5 M NaCl) turns out to be ~22. To the best of our knowledge, these results constitute one of the early reports on polarity estimates in rod-shaped micelles. In addition, pyrene excimer/monomer ratio shows increase in SDS micelles with increasing NaCl concentration. We interpret this increase due to an increase in average number of pyrene molecules per micelle associated with the sphere-to-rod structural transition. These results could be significant in micellar drug solubilization and delivery, and in membrane morphology changes.

Introduction

Detergents are crucial in studies of biological membranes due to their ability to solubilize membrane proteins and receptors [1,2]. They are soluble amphiphiles and above a critical concentration (strictly speaking, a narrow concentration range), known as the critical micelle concentration (CMC), self-associate to form thermodynamically stable, noncovalent aggregates called micelles, at temperatures above the critical micelle temperature (CMT) [3]. Micelles are widely used as membrane mimetic systems to characterize membrane proteins and peptides [4] and as vehicles for drug delivery [5]. Studies on micellar organization and dynamics assume significance in light of the fact that the general principle underlying the formation of micelles (i.e., the hydrophobic effect) is common to other related assemblies such as reverse micelles, bilayers, liposomes, and biological membranes [6,7]. Micelles are highly cooperative, organized molecular assemblies of amphiphiles, yet dynamic in nature. In addition, they offer certain inherent advantages in fluorescence studies over membranes since micelles are smaller and optically transparent, have well-defined sizes, and are relatively scatter-free. Micelles can be of any desired charge type and can adopt different shapes and internal packing, depending on the chemical structures of the constituent monomers and the ionic strength of the medium [8–11].

Structural transition can be induced in charged micelles at a given temperature by increasing ionic strength of the medium or amphiphile concentration [8–10,12–14]. For example, spherical micelles of sodium dodecyl sulfate (SDS) that exist in water at concentrations higher than CMC assume an elongated rod-like (prolate) structure in presence of high electrolyte (salt) concentrations when interactions among the charged headgroups are attenuated due to the added salt (see Fig. 1). This is known as sphere-to-rod transition [15]. This shape change induced by increased salt concentration is accompanied by a reduction in CMC [16]. It has been suggested that large rod-shaped micelles are better models for biomembranes [17] perhaps due to the release of curvature stress encountered in spherical micelles, and the hydrocarbon chains are more ordered in rod-shaped micelles compared to spherical micelles [12]. Micellar sphere-to-rod transition can be explained in terms of the packing model described by Israelachvili [18]. In this paper, we have monitored the change in organization and dynamics associated with sphere-to-rod transition of SDS micelles utilizing pyrene fluorescence.

Abbreviations: CMC, critical micelle concentration; CMT, critical micelle temperature; SDS, sodium dodecyl sulfate; DPH, 1,6-diphenyl-1,3,5-hexatriene.

* Corresponding author. Fax: +91 40 2716 0311.
E-mail address: amit@ccmb.res.in (A. Chattopadhyay).

0006-291X/$ - see front matter © 2009 Elsevier Inc. All rights reserved.
doi:10.1016/j.bbrc.2009.10.037

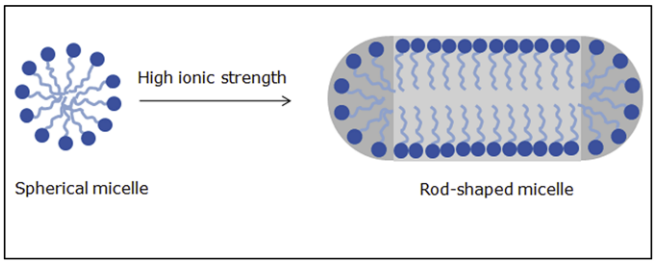

Fig. 1. A schematic representation of the sphere-to-rod transition in charged SDS micelle induced by high ionic strength. The transition of micelle shape from sphere to rod takes place in SDS at concentrations well above the critical micelle concentration, when salt (NaCl) concentration is higher than 0.45 M [10]. The microenvironment and packing for micelle-bound molecules in rod-shaped micelles are heterogeneous and are shown as spherical 'end caps' (darker shade) and the cylindrical central part (lighter shade). Note that the headgroup spacing is reduced in the cylindrical part of the rod shaped micelle due to attenuation of interactions among the charged head groups induced by high ionic strength.

Materials and methods

Materials. SDS, pyrene, and NaCl were purchased from Sigma Chemical Co. (St. Louis, MO). DPH was obtained from Molecular Probes (Eugene, OR). The purity of SDS was checked by measuring its CMC and comparing with literature CMC. CMC of SDS was determined fluorimetrically utilizing the enhancement of DPH fluorescence upon micellization [16]. The concentration of the stock solution of pyrene in methanol was estimated from its molar extinction coefficient of 54,000 $M^{-1}cm^{-1}$ at 335 nm [19]. Solvents (methanol, ethanol, *n*-propanol, *n*-butanol, *n*-hexanol, and *n*-octanol) used were of spectroscopic grade. Water was purified through a Millipore (Bedford, MA) Milli-Q system and used throughout.

Sample preparation. The concentration of SDS (16 mM) used was double its CMC, to ensure that it is in the micellar state in all experiments. The molar ratio of pyrene to SDS was carefully chosen [1:500 (mol/mol)] to give optimum signal-to-noise ratio with minimal perturbation to the micellar organization and negligible interprobe interactions. In order to incorporate pyrene into micelles, a small aliquot containing 48 nmol of pyrene from a methanol stock solution was added to 1.5 ml of preformed micelles (containing varying amounts of NaCl) and mixed well by vortexing for 3 min. The resultant pyrene concentration was 32 μM in all cases and the methanol content was always low (<0.25% v/v). Background samples were prepared in the same way except that pyrene was not added to them. Samples were equilibrated in the dark for 12 h before measuring fluorescence. Since the CMT of SDS in presence of 0.5 M NaCl (highest concentration of NaCl used) is 24.7 °C [10], all sample preparations and experiments were performed at 25 °C.

Fluorescence spectroscopic measurements. Steady state fluorescence measurements of samples containing pyrene were performed with a Hitachi F-4010 spectrofluorometer using 1 cm path length quartz cuvettes. For measuring pyrene fluorescence, samples were excited at 335 nm. Excitation and emission slits with a nominal bandpass of 3 nm were used for all measurements. The background intensities of samples in which pyrene was omitted were negligible in most cases and were subtracted from each sample spectrum to cancel out any contribution due to the solvent Raman peak and other scattering artifacts. Due to relatively small size of micelles, samples were relatively scatter-free. The ratio of the first (373 nm) and third (384 nm) vibronic peak intensities (I_1/I_3) was calculated from pyrene emission spectra. The excimer/monomer fluorescence intensity ratio was determined by measuring the fluorescence intensity at the monomer (393 nm) and excimer (480 nm) peaks.

Results and discussion

In this work, we have used the hydrophobic membrane probe pyrene to explore the change in organization and dynamics associated with sphere-to-rod transition of SDS micelles. The fluorescence emission spectrum of pyrene is sensitive to environmental polarity [20]. Pyrene also forms excimers with very different fluorescence characteristics and the ratio of excimer/monomer is known to be dependent on host dynamics [21,22]. It has been previously shown that pyrene is localized predominantly in the interfacial region in micelles [23–25]. This is consistent with the observation that practically all types of molecules (aromatic molecules in particular) have a surface-seeking tendency in micelles (due to very large surface area to volume ratio) and the interfacial region is the preferred site for solubilization, even for hydrophobic molecules [24,26]. Interestingly, this is the region of the micelle that is sensitive to polarity changes due to water penetration (see later).

Fluorescence emission spectra of pyrene in spherical and rod-shaped micelles are shown in Fig. 2. A characteristic feature of the structured spectra is the emission maxima at 373, 384 and 393 nm. This type of structured vibronic band intensities, displayed by fluorophores such as pyrene [20] and dehydroergosterol [27], are known to be environmentally sensitive. This property has previously been effectively used for elucidating microenvironments of pyrene [22,28,29]. The ratio of the first (373 nm) and third (384 nm) vibronic peak intensities (I_1/I_3) in pyrene emission spectrum provides a measure of the apparent polarity of the environment. An increase in the ratio is indicative of increased polarity.

The change in the ratio of vibronic peak intensities (I_1/I_3) in pyrene emission spectra in SDS micelles with increasing concentrations of NaCl is shown in Fig. 3A. The figure shows that increasing ionic strength resulted in a reduction in the vibronic peak intensity ratio. This could imply a decrease in apparent polarity experienced by pyrene in SDS micelles in presence of NaCl, possibly due to a reduction in micellar water content accompanying shape transition in presence of NaCl (or deeper localization of pyrene in rod-shaped micelles). In presence of NaCl, the electrostatic repulsion between negatively charged headgroups of SDS is attenuated due to shielding (screening) of charges, thereby reducing

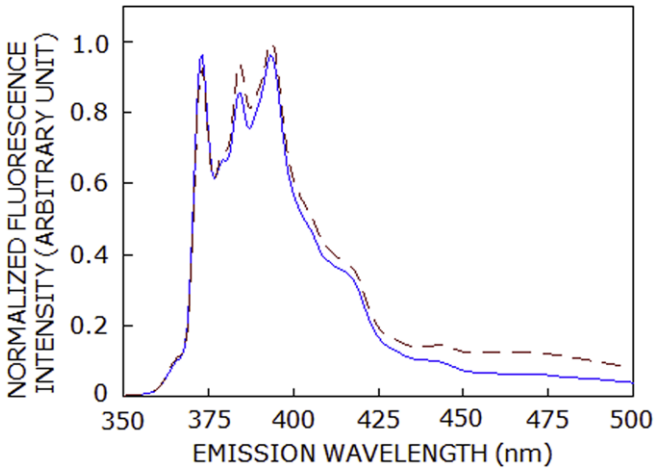

Fig. 2. Representative fluorescence emission spectra of pyrene in SDS micelles in the absence (blue solid line), and presence (red broken line) of 0.5 M NaCl. Spectra are intensity-normalized at the respective emission maximum. Measurements were carried out at 25 °C. The excitation wavelength used was 335 nm. The ratio of pyrene to SDS was 1:500 (mol/mol), and the concentration of SDS was 16 mM. See Materials and methods for other details. (For interpretation of the references to color in this figure legend, the reader is referred to the web version of this paper.)

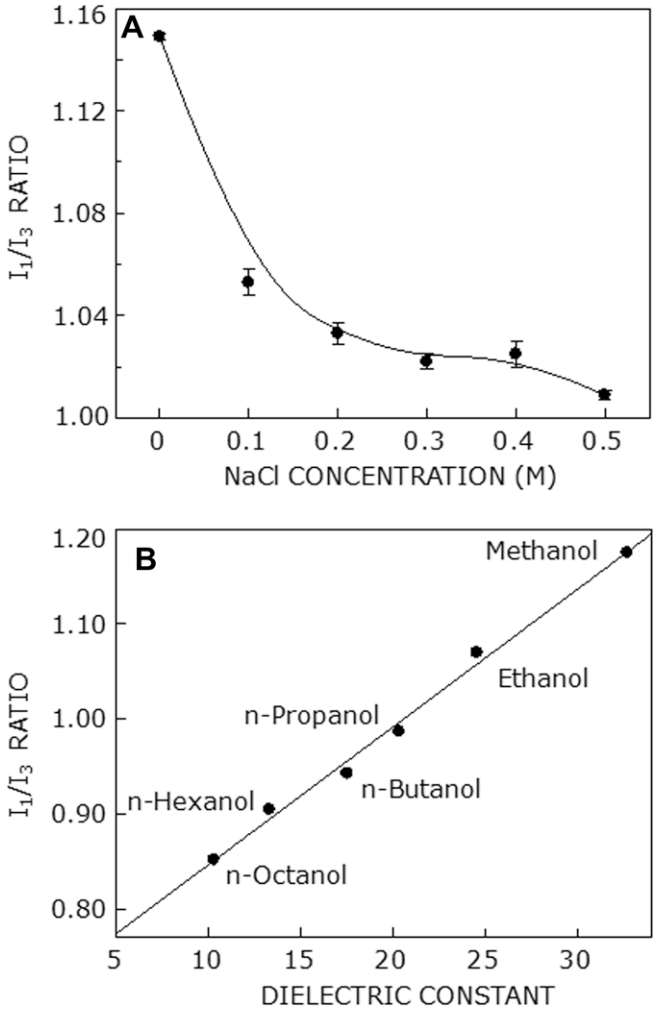

Fig. 3. (A) Change in fluorescence intensity ratio of the first (373 nm) and third (384 nm) vibronic peaks of pyrene (I_1/I_3) in SDS micelles as a function of increasing concentration of NaCl. Data points are means ± SE of at least four independent measurements. The line joining the data points is provided merely as a viewing guide. The ratio of pyrene to SDS was 1:500 (mol/mol), and the concentration of SDS was 16 mM. (B) Calibration plot between the fluorescence intensity ratio of the first (373 nm) and the third (384 nm) vibronic peaks of pyrene (I_1/I_3) and static dielectric constant (ϵ) of various alcohols at 25 °C, ranging between 10.3 (*n*-octanol) and 32.6 (methanol) taken from [49]. The calibration plot indicates an excellent linear correlation ($y = 0.0145x + 0.7022$; $r = 0.99$) between the ratio I_1/I_3 and the static dielectric constant of various alcohols. See Materials and methods for other details.

surface area per headgroup (see Fig. 1) which results in less water penetration in the interfacial region.

In order to obtain an estimate of the decrease in apparent polarity experienced by pyrene in SDS micelles with NaCl concentration, we utilized the linear relationship between the ratio of the vibronic peak intensities (I_1/I_3) and dielectric constant (ϵ) [27–29]. Fig. 3B shows the calibration plot between I_1/I_3 and static dielectric constant of various alcohols ranging from 10.3 to 32.6. Since the only polar group in these alcohols is the hydroxyl group, the I_1/I_3 ratio corresponding to each one of them can be attributed to their relative polarity. A higher value of I_1/I_3 corresponds to a relatively polar solvent (such as methanol) while a lower value of I_1/I_3 corresponds to a relatively nonpolar solvent (such as *n*-octanol). We utilized this calibration plot in order to gain information on the apparent polarity experienced by pyrene in SDS micelles with increasing NaCl concentration. The apparent dielectric constants derived from the calibration plot (Fig. 3B) are summarized in Table 1. The apparent dielectric constant experienced by pyrene in

Table 1
Apparent dielectric constants (ϵ) determined from pyrene vibronic peak intensity ratio (I_1/I_3) measurements[a].

Experimental condition (NaCl concentration)	Dielectric constant (ϵ)
0	32.00
0.1 M	25.14
0.2 M	23.71
0.3 M	22.93
0.4 M	23.14
0.5 M	22.00

[a] The concentration of SDS was 16 mM in all cases. The dielectric constant was obtained from the calibration plot shown in Fig. 3B using I_1/I_3 values from pyrene vibronic peak intensities in the emission spectra. The first (373 nm) and third (384 nm) vibronic peak intensity ratio (I_1/I_3) of pyrene under different conditions is from Fig. 3A. The concentration of pyrene was 32 μM and the ratio of pyrene to SDS was 1:500 (mol/mol). See Materials and methods for other details.

spherical SDS micelles (in the absence of NaCl) is ~32. As is evident from the table, the apparent dielectric constant experienced by pyrene displays a reduction with increasing NaCl concentration. This reinforces our earlier conclusion from Fig. 3A. The dielectric constant experienced by pyrene in rod-shaped micelles of SDS (in presence of 0.5 M NaCl) turns out to be ~22. To the best of our knowledge, these results constitute one of the early reports on change in dielectric constant of SDS micelles upon shape transition induced by high ionic strength.

A commonly used parameter related to pyrene fluorescence is the excimer/monomer fluorescence intensity ratio [21,22]. This parameter is indicative of the extent of pyrene excimerization that is believed to depend on the monomer lateral distribution and dynamics (diffusion) in the host assembly, although the exact mechanism of excimerization is not clear [30]. Fig. 4 shows the excimer/monomer ratio in SDS micelles with increasing NaCl concentration, with a sharp increase at high NaCl concentrations. The extent of excimer formation appears to increase with increase in salt concentration. It has been proposed that excimer formation in micelles is determined by the rate of diffusion of pyrene and the distribution of the probe among the micelles [31]. In relatively small SDS spherical micelles (at low NaCl concentration), a fraction of micelles will have more than one pyrene molecule incorporated

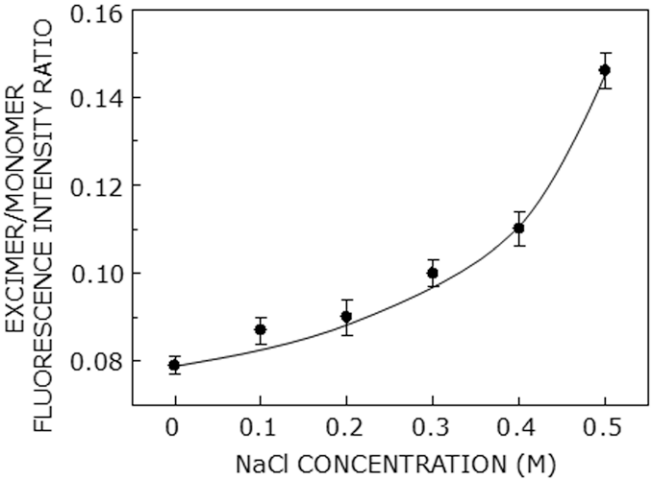

Fig. 4. Pyrene excimer (480 nm)/monomer (393 nm) fluorescence intensity ratio in SDS micelles as a function of increasing concentration of NaCl. Data points are means ± SE of at least four independent measurements. The line joining the data points is provided merely as a viewing guide. The ratio of pyrene to SDS was 1:500 (mol/mol) and the concentration of SDS was 16 mM. See Materials and methods for other details.

in them. This fraction will contribute to the excimer/monomer fluorescence intensity ratio since the intermicellar exchange of pyrene is slow with respect to the fluorescence lifetime of pyrene (pyrene has a long lifetime, typically ~300 ns in SDS micelles [32]). The distribution of probes in micelles is determined by Poisson statistics [33]. If x is the ratio of concentrations of the probe to micelles such as x = [probe]/[micelles], the probability distribution is given by:

$$P(n) = x^n e^{-x}/n!$$

where $P(n)$ represents the probability that a micelle is occupied by n probe molecules (n is the number of probe molecules per micelle). The concentration of micelles can be calculated from:

$$[\text{micelles}] = (S - \text{CMC})/N$$

where S is the concentration of surfactant, and N is the aggregation number. Using this formalism, we calculated that for spherical SDS micelles (in absence of salt) the probability of more than one pyrene molecule present (*necessary condition for excimer formation*) in a micelle is ~3% (assuming a CMC of 8.2 mM [3] and aggregation number of 62 [3]). The same calculation, in case of rod-shaped SDS micelles yields a probability of ~26% for the presence of more than one pyrene molecule per micelle (assuming a CMC of 0.5 mM [34] and aggregation number of 480 [8]). Thus, there is an increase in average number of pyrene molecules per micelle associated with the sphere-to-rod structural transition that is reflected in the increase the excimer/monomer ratio.

A comparison of the dependence of I_1/I_3 and excimer/monomer ratio on ionic strength merits comment. The I_1/I_3 ratio displays sharp reduction with the addition of 0.1 M NaCl, followed by less appreciable change with increasing salt concentration (Fig. 3A). In contrast, the excimer/monomer ratio exhibits a sharp increase between 0.4 and 0.5 M NaCl (Fig. 4), the concentration range where the shape change has been reported to occur [9]. The reduction in I_1/I_3 ratio at low ionic strength could be due to decrease in micellar water content. The geometry and packing features of spherical micelles are somewhat loose [35] that allows more water penetration into the micellar interior [23]. Upon addition of NaCl, there is a decrease in headgroup spacing due to screening of headgroup charges, thereby inducing tighter packing of detergent monomers in the micellar assembly. This results in a reduction in micellar water content, as evident by decrease in I_1/I_3 ratio. This enables more monomers to pack in each micelle that ultimately results in shape change at higher ionic strength.

Structural transitions involving shape changes play an important role in cellular physiology [36]. For example, the shape of erythrocytes (red blood cells) has been shown to change with the pH and ionic strength of the medium [37]. The shape of the erythrocyte is believed to be maintained by the membrane skeleton in close interaction with the plasma membrane [38]. Investigations into the role of the membrane in such shape changes have revealed that modification of either the membrane composition or the structure of its individual constituents can lead to shape changes [39]. Alteration of cholesterol level, selective removal of phospholipids from the outer membrane leaflet, pH and membrane potential alterations, metabolic depletion, and introduction of lysophospholipids, fatty acids, and charged amphipathic agents in membranes leads to shape changes of erythrocytes [39–41]. Shape changes can be induced even in liposomes by mechanical stress, temperature or pH variation, osmotic shock, and by asymmetric transmembrane distribution of phospholipids [42]. Shape changes in cellular membranes that occur due to modifications of membrane composition [39–41] can directly affect the function of membrane proteins such as mechanosensitive channels that respond to changes in membrane curvature [43]. For example, the function of the gramicidin channel has been shown to be sensitive to curvature changes of the membrane bilayer [44]. Interestingly, SDS micellar shape change induced by chlorpromazine, an amphiphilic cationic phenothiazine drug, has been reported [45].

In this paper, we have explored the changes in organization and dynamics associated with the salt-induced sphere-to-rod structural transition in charged micellar assemblies by monitoring changes in pyrene fluorescence. Our results show that the polarity of the micellar interface, as experienced by pyrene, is reduced upon structural transition to rod-shaped micelles (Table 1). Interestingly, the apparent dielectric constant reported here for rod-shaped micelles compares well with the apparent polarity of hippocampal [46] and model [47] membranes. This reinforces the proposition that the rod-shaped micelles have an organization of amphiphiles similar to that of a bilayer and therefore are better models for membrane bilayers [17,31]. Interestingly, micellar polarity (dielectric constant) plays an important role in the incorporation (solubilizing capacity) of drugs [48]. The difference in organization of spherical and rod-shaped micelles, as reported here using pyrene fluorescence, could have implications in conformation of membrane proteins and peptides. For example, it has been recently reported that the conformation and dynamics of the ion channel gramicidin is sensitive to structural changes in the host assembly [14].

Acknowledgments

This work was supported by the Council of Scientific and Industrial Research (Government of India) Network project on Nanomaterials and Nanodevices (NWP0035). Ar.C. and S.H. thank the Council of Scientific and Industrial Research for the award of Research Fellowships. We thank Sandeep Shrivastava for useful discussion. A.C. is an Adjunct Professor at the Special Centre for Molecular Medicine of Jawaharlal Nehru University (New Delhi, India), and Honorary Professor at the Jawaharlal Nehru Centre for Advanced Scientific Research (Bangalore, India). A.C. gratefully acknowledges support from J.C. Bose Fellowship (Department of Science and Technology, Govt. of India). We dedicate this paper to the memory of Prof. Meenakshi Mukherjee, and thank members of our laboratory for critically reading the manuscript.

References

[1] A. Chattopadhyay, K.G. Harikumar, S. Kalipatnapu, Solubilization of high affinity G-protein-coupled serotonin$_{1A}$ receptors from bovine hippocampus using pre-micellar CHAPS at low concentration, Mol. Membr. Biol. 19 (2002) 211–220.
[2] A.M. Seddon, P. Curnow, P.J. Booth, Membrane proteins, lipids and detergents: not just a soap opera, Biochim. Biophys. Acta 1666 (2004) 105–117.
[3] A. Helenius, K. Simons, Solubilization of membranes by detergents, Biochim. Biophys. Acta 415 (1975) 29–79.
[4] S.S. Sham, S. Shobana, L.E. Townsley, J.B. Jordan, J.Q. Fernandez, O.S. Andersen, D.V. Greathouse, J.F. Hinton, The structure, cation binding, transport and conductance of Gly$_{15}$-gramicidin A incorporated into SDS micelles and PC/PG vesicles, Biochemistry 42 (2003) 1401–1409.
[5] A.S. Narang, D. Delmarre, D. Gao, Stable drug encapsulation in micelles and microemulsions, Int. J. Pharm. 345 (2007) 9–25.
[6] C. Tanford, The hydrophobic effect and the organization of living matter, Science 200 (1978) 1012–1018.
[7] J.N. Israelachvili, S. Marcelja, R.G. Horn, Physical principles of membrane organization, Q. Rev. Biophys. 13 (1980) 121–200.
[8] N.A. Mazer, G.B. Benedek, M.C. Carey, An investigation of the micellar phase of sodium dodecyl sulfate in aqueous sodium chloride solutions using quasielastic light scattering spectroscopy, J. Phys. Chem. 80 (1976) 1075–1086.
[9] C.Y. Young, P.J. Missel, N.A. Mazer, G.B. Benedek, M.C. Carey, Deduction of micellar shape from angular dissymmetry measurements of light scattered from aqueous sodium dodecyl sulfate solutions at high sodium chloride concentrations, J. Phys. Chem. 82 (1978) 1375–1378.
[10] S. Hayashi, S. Ikeda, Micelle size and shape of sodium dodecyl sulfate in concentrated NaCl solutions, J. Phys. Chem. 84 (1980) 744–751.
[11] H. Raghuraman, A. Chattopadhyay, Effect of micellar charge on the conformation and dynamics of melittin, Eur. Biophys. J. 33 (2004) 611–622.

[12] H.A. Heerklotz, A. Tsamaloukas, K. Kita-Tokarczyk, P. Strunz, T. Gutberlet, Structural, volumetric, and thermodynamic characterization of a micellar sphere-to-rod transition, J. Am. Chem. Soc. 126 (2004) 16544–16552.
[13] Y. Geng, L.S. Romsted, S. Froehner, D. Zanette, L.J. Magid, I.M. Cuccovia, H. Chaimovich, Origin of the sphere-to-rod transition in cationic micelles with aromatic counterions: specific ion hydration in the interfacial region matters, Langmuir 21 (2005) 562–568.
[14] S.S. Rawat, D.A. Kelkar, A. Chattopadhyay, Effect of structural transition of the host assembly on dynamics of an ion channel peptide: a fluorescence approach, Biophys. J. 89 (2005) 3049–3058.
[15] P.J. Missel, N.A. Mazer, M.C. Carey, G.B. Benedek, Thermodynamics of the sphere-to-rod transition in alkyl sulfate micelles, in: K.L. Mittal, E.J. Fendler (Eds.), Solution Behavior of Surfactants: Theoretical and Applied Aspects, Vol. 1, Plenum Press, New York, 1984, pp. 373–388.
[16] A. Chattopadhyay, E. London, Fluorimetric determination of critical micelle concentration avoiding interference from detergent charge, Anal. Biochem. 139 (1984) 408–412.
[17] S.S. Rawat, A. Chattopadhyay, Structural transition in the micellar assembly: a fluorescence study, J. Fluoresc. 9 (1999) 233–244.
[18] J.N. Israelachvili, Intermolecular and Surface Forces, second ed., Academic Press, London, 1991.
[19] I.B. Berlman, Handbook of Fluorescence Spectra of Aromatic Molecules, Academic Press, New York, 1971.
[20] D.C. Dong, M.A. Winnik, The *Py* scale of solvent polarities. Solvent effects on the vibronic fine structure of pyrene fluorescence and empirical correlations with E_T and *Y* values, Photochem. Photobiol. 35 (1982) 17–21.
[21] J.M. Vanderkooi, J.B. Callis, Pyrene: a probe of lateral diffusion in the hydrophobic region of membranes, Biochemistry 3 (1974) 4000–4006.
[22] V. Ioffe, G.P. Gorbenko, Lysozyme effect on structural state of model membranes as revealed by pyrene excimerization studies, Biophys. Chem. 114 (2005) 199–204.
[23] F.M. Menger, On the structure of micelles, Acc. Chem. Res. 12 (1979) 111–117.
[24] J. Shobha, V. Srinivas, D. Balasubramanian, Different modes of incorporation of probe molecules in micelles and in bilayer vesicles, J. Phys. Chem. 93 (1989) 17–20.
[25] R. Konuk, J. Cornelisse, S.P. McGlynn, Fluorescence quenching of pyrene by Cu^{2+} and Co^{2+} in sodium dodecyl sulfate micelles, J. Phys. Chem. 93 (1989) 7405–7408.
[26] P. Mukerjee, J.R. Cardinal, Benzene derivatives and naphthalene solubilized in micelles. Polarity of microenvironment, location and distribution in micelles, and correlation with surface activity in hydrocarbon-water systems, J. Phys. Chem. 82 (1978) 1620–1627.
[27] R. Rukmini, S.S. Rawat, S.C. Biswas, A. Chattopadhyay, Cholesterol organization in membranes at low concentrations: effects of curvature stress and membrane thickness, Biophys. J. 81 (2001) 2122–2134.
[28] N.J. Turro, P.-L. Kuo, P. Somasundaran, K. Wong, Surface and bulk interactions of ionic and non ionic surfactants, J. Phys. Chem. 90 (1986) 288–291.
[29] M.E. Haque, S. Ray, A. Chakrabarti, Polarity estimate of the hydrophobic binding sites in erythroid spectrin: a study by pyrene fluorescence, J. Fluoresc. 10 (2000) 1–6.
[30] M.F. Blackwell, K. Gounaris, J. Barber, Evidence that pyrene excimer formation in membranes is not diffusion-controlled, Biochim. Biophys. Acta 858 (1986) 221–234.
[31] K. Kalyanasundaram, M. Gratzel, J.K. Thomas, Electrolyte-induced phase transitions in micellar systems. A proton and carbon-13 nuclear magnetic resonance relaxation and photochemical study, J. Am. Chem. Soc. 97 (1975) 3915–3922.
[32] A. Siemiarczuk, W.R. Ware, Pyrene lifetime broadening in SDS micelles, Chem. Phys. Lett. 167 (1990) 263–268.
[33] N.J. Turro, P.-L. Kuo, Excimer formation of a water-soluble fluorescence probe in anionic micelles and nonionic polymer aggregates, Langmuir 3 (1987) 773–777.
[34] C. Tanford, The hydrophobic effect: formation of micelles and biological membranes, John Wiley, New York, 1980. p. 67.
[35] D.W.R. Gruen, A model for the chains in amphiphilic aggregates. 2. Thermodynamic and experimental comparisons for aggregates of different shape and size, J. Phys. Chem. 89 (1985) 153–163.
[36] E. Paluch, C.-P. Heisenberg, Biology and physics of cell shape changes in development, Curr. Biol. 19 (2009) R790–R799.
[37] M. Rasia, A. Bollini, Red blood cell shape as a function of medium's ionic strength and pH, Biochim. Biophys. Acta 1372 (1998) 198–204.
[38] E.J. Luna, A.L. Hitt, Cytoskeleton–plasma membrane interactions, Science 258 (1992) 955–963.
[39] F.A. Kuypers, B. Roelofsen, W. Berendsen, J.A.F. Op den Kamp, L.L.M. van Deenen, Shape changes in human erythrocytes induced by replacement of the native phosphatidylcholine with species containing various fatty acids, J. Cell Biol. 99 (1984) 2260–2267.
[40] L. Backman, J.B. Jonasson, P. Hörstedt, Phosphoinositide metabolism and shape control in sheep red blood cells, Mol. Membr. Biol. 15 (1998) 27–32.
[41] M.M. Gedde, W.H. Huestis, Membrane potential and human erythrocyte shape, Biophys. J. 72 (1997) 1220–1233.
[42] E. Farge, P.F. Devaux, Shape changes of giant liposomes induced by an asymmetric transmembrane distribution of phospholipids, Biophys. J. 61 (1992) 347–357.
[43] E. Perozo, A. Kloda, D.M. Cortes, B. Martinac, Physical principles underlying the transduction of bilayer deformation forces during mechanosensitive channel gating, Nat. Struct. Biol. 9 (2002) 696–703.
[44] J.A. Lundbaek, A.M. Maer, O.S. Andersen, Lipid bilayer electrostatic energy, curvature stress, and assembly of gramicidin channels, Biochemistry 36 (1997) 5695–5701.
[45] W. Caetano, E.L. Gelamo, M. Tabak, R. Itri, Chlorpromazine and sodium dodecyl sulfate mixed micelles investigated by small angle X-ray scattering, J. Colloid Interface Sci. 248 (2002) 149–157.
[46] R. Saxena, S. Shrivastava, A. Chattopadhyay, Exploring the organization and dynamics of hippocampal membrane utilizing pyrene fluorescence, J. Phys. Chem. B 112 (2008) 12134–12138.
[47] S. Shrivastava, Y.D. Paila, A. Dutta, A. Chattopadhyay, Differential effects of cholesterol and its immediate biosynthetic precursors on membrane organization, Biochemistry 47 (2008) 5668–5677.
[48] T. Rebagay, P. Deluca, Correlation of dielectric constant and solubilizing properties of tetramethyldicarboxamides, J. Pharm. Sci. 65 (2006) 1645–1648.
[49] D.R. Lide (Ed.), CRC Handbook of Chemistry and Physics, CRC Press, Boca Raton, FL, 1992.